Paper No. 00-1517

Effects of Relaxation and Anticipation on Riemann Solutions of Payne-Whitham Model

H. M. Zhang and T. Kim

The solutions of Riemann problems of a particular higher-order model—the Payne-Whitham (PW) model—are studied using Roe's flux splitting scheme as presented by Leo and Pretty. Despite numerous works on higher-order models, little is known about Riemann solutions of these models and how relaxation and anticipation affect these solutions. Riemann solutions of the PW model are computed and compared with those of the Lighthill-Whitham-Richards (LWR) model having the same initial (density) data. It was found that faster relaxation forces the PW model to behave much like the LWR model, that strong anticipation has a stabilizing effect on traffic, and that shock waves travel at different speeds in the PW model than they do in the LWR model. These findings provide a basic checklist for experimental validation of PW-like higher models.

With the exception of the kinematic wave model of Lighthill and Whitham (*1*) and Richards (*2*) (LWR), perhaps no other model in traffic flow has been so widely studied and used than the higher-order continuum model of Payne (*3*, pp. 51–60) and Whitham (*4*) (PW). Experiences in applying the PW model, however, are not equally satisfying. Although some researchers obtained excellent results fitting this model to real-world data [e.g., Papageorgiou (*5*) and Papageorgiou et al. (*6*)], others encountered great difficulty in applying it to traffic bottlenecks [e.g., Hauer and Hurdle (*7*) and Derzko et al. (*8*)]. Although a flaw in the PW model [i.e., wrong-way travel (*9*)] may have contributed to this difficulty, it is suspected that the difficulty was largely caused by the primitive numerical schemes used to approximate the PW model. These schemes use simple forward and backward differences in their approximations of the PW equations, and the solutions they produce may not converge to the true PW solutions. It was not until the work of Leo and Pretty (*10*) that more refined and accurate finite difference approximations of the PW model were first used in traffic simulations. Leo and Pretty showed that the PW model produces satisfactory results for freeway traffic flowing through a bottleneck (lane drop) and models flow on an arterial link equally as well as the LWR model does. They also noted, however, that the PW model did not produce "more realistic results."

The latter revelation was not surprising because upon examination of the parameters used in their work (*10*), it was found that a "small" relaxation time ($\tau = 1$ s) was used. When relaxation is fast, the PW model approaches the "viscous" LWR model asymptotically (i.e., the continuity equation with an additional source term that contains the second-order derivative of density with respect to distance) (*11*). On the other hand, this observation led the authors to wonder how the PW solutions differ from the LWR solutions when τ is not small, and how other factors, namely, driver anticipation, contribute to this difference.

Because Leo and Pretty (*10*) used complex initial and boundary data in their simulations, the answers to the aforementioned questions cannot be readily inferred from their work. In this study the answer to these questions is sought by studying the Riemann problems of the PW model using the finite difference scheme developed by Leo and Pretty (*10*). The basic background of both PW and LWR models and their Riemann problems is given in the next section. Then the Godunov finite difference for the LWR model and Roe's flux splitting difference for the PW model are given, followed by the Riemann initial data and the corresponding numerical results.

Department of Civil and Environmental Engineering, University of California, Davis, Davis, CA 95616.

CONTINUUM MODELS AND RIEMANN PROBLEMS

Let x denote space, t time, q flow rate, ρ vehicle concentration (density), and v travel speed. Fundamental to any continuum theory are three equations:

Conservation of vehicles:

$$\rho_t + q_x = 0 \tag{1}$$

Flow equation:

$$q = \rho v \tag{2}$$

Equation of state of stationary (or equilibrium) flow:

$$v = v_*(\rho) \tag{3}$$

where $v_*(\rho)$ is a nonincreasing and smooth function of ρ.

Equation 1 derives from physical principles, Equation 2 from variable definitions, and Equation 3 from empirical observations. As such, the only element that distinguishes traffic flow from material flow is Equation 3. Consequently, it is also the diverging point of various continuum models. If one insists that Equation 3 is valid for general flow, one obtains the LWR model:

$$\rho_t + f_*'(\rho)\rho_x = 0 \tag{4}$$

where $f_*'(\rho) = (\rho v_*)'$ is given a name "wave" or "characteristic" velocity, and the prime denotes total derivative. Furthermore, there is a critical density ρ_* such that $f_*(\rho_*) \geq f_*(\rho)$. In other words, flow reaches capacity at critical density.

On the other hand, if one believes that Equation 3 gives only a rough cut of traffic behavior and some fine-tuning is required to take account of driver anticipation, one can use the PW model. In addition to the conservation equation, the PW model also contains a more complex equation to describe speed dynamics:

$$v_t + vv_x + \frac{c_0^2}{\rho}\rho_x = \frac{v_*(\rho) - v}{\tau} \tag{5}$$

where τ is the relaxation time, and c_0 is traffic "sound" speed. The magnitude of c_0 reflects how strongly drivers anticipate and react to traffic conditions ahead of them.

It turns out that both models comprise hyperbolic partial differential equations (PDEs), with the LWR model a single PDE and the PW model a system of PDEs. As such, discontinuous solutions, called shocks, arise from even smooth initial data in these models. A particular problem, called a Riemann problem, is often used to characterize the solutions of hyperbolic PDEs. A Riemann problem is nothing more than hyperbolic PDEs with a special set of initial data, called Riemann data, in which a single jump discontinuity separates two infinitely long regions of constant states (e.g., ρ, v, q). Riemann data for the LWR model, for example, are as follows:

$$\rho(x, 0) = \begin{cases} \rho_l, & x < 0 \\ \rho_r, & x \geq 0 \end{cases}$$

where ρ_l and ρ_r are two constants.

The solutions to hyperbolic PDEs with Riemann initial data, called Riemann solutions, are usually of three basic types: shocks, rarefaction waves, and contacts (*12*). Not every one of these waves is present in the LWR and PW models. Contacts, for example, do not exist in either model. Because of the existence of shocks, hyperbolic PDEs such as those of the LWR and PW models are notoriously difficult to solve numerically. Special care must be taken when these equations are converted into finite difference equations (FDEs), which will be discussed in the next section.

FINITE DIFFERENCE APPROXIMATIONS

Finite difference schemes divide the continuous time-space domain into a mesh of grid points, with each point being the center of a cell representing a segment of road (Figure 1). The quantities of a cell (i, j), ρ_i^j and v_i^j, represent the average cell density and speed, respectively, at location $(i - \frac{1}{2})h < x \leq (i - \frac{1}{2})h$ and time $t_j = jk$ (here h is the cell length and k is the time increment); that is,

$$\rho_i^j = \frac{1}{h}\int_{(j-1/2)^h}^{(j+1/2)^h} \rho(x, t_j)dx \qquad v_i^j = \frac{1}{h}\int_{(j-1/2)^h}^{(j+1/2)^h} v(x, t_j)dx$$

As the mesh is refined (i.e., $h \to 0$, $k \to 0$, and h/k = constant), ρ_i^j and v_i^j are expected to approach the true solutions $\rho(x_i, t_j)$ and $v(x_i, t_j)$, respectively, if the finite difference is correct.

Because of their admittance to shocks, nonlinear hyperbolic PDEs such as the ones in traffic flow are notoriously difficult to solve numerically. Many straightforward finite difference approximations, such as forward difference or center difference approximations, of these PDEs often fail miserably. If these PDEs can be written in a particular form, called the conservative form, some rather well-established finite difference schemes could be used to solve them numerically. These schemes include Godunov's scheme (*13*) and Roe's flux splitting scheme (*14*). The former and its variations have been used to solve the LWR model by a number of authors (*15–17*), whereas the latter was applied to solve the PW model by Leo and Pretty (*10*).

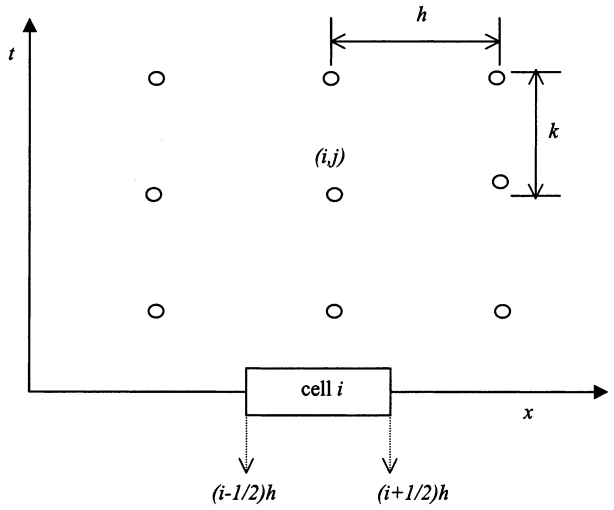

FIGURE 1 Finite difference mesh.

Let U denote the state variable (U = [ρ] for LWR and

$$U = \begin{bmatrix} \rho \\ \rho v \end{bmatrix}$$

for PW); the conservative form of both LWR and PW models is

$$U_t + F(U)_x = s(U) \tag{6}$$

The flux functions and source fluxes are

$$F(U) = f_*(\rho) \qquad s(U) = 0$$

for the LWR model, and

$$F(U) = \begin{pmatrix} \rho v \\ \rho v^2 + \rho c_0^2 \end{pmatrix}, \quad s(U) = \begin{pmatrix} 0 \\ \dfrac{\rho(v_*(\rho) - v)}{\tau} \end{pmatrix}$$

for the PW model.

The Godunov scheme for Equation 6 is as follows:

$$U_i^{j+1} = U_i^j - \frac{k}{h}\left[F(U_i^j, U_{i+1}^j) - F(U_{i-1}^j, U_i^j)\right]$$

where $F(U_i^j, U_{i+1}^j)$ is called the numerical flux. When Equation 6 is of a single PDE (i.e., the LWR model), it is computed by

$$F(U_i^j, U_{i+1}^j) = \max(D_i^j, S_{i+1}^j)$$

That is, the minimum of the local supply of cell $i + 1$ and local demand of cell i. The demand and supply functions are defined as follows (*16*, *17*):

$$\text{Demand: } D(i, j) = \begin{cases} f_*(\rho_i^j) & \text{if } \rho_i^j < \rho_* \\ f_*(\rho_*) & \text{if } \rho_i^j \geq \rho_* \end{cases}$$

$$\text{Supply: } S(i,j) = \begin{cases} f_*(\rho_i^j) & \text{if } \rho_i^j > \rho_* \\ f_*(\rho_*) & \text{if } \rho_i^j \le \rho_* \end{cases}$$

The Godunov scheme for the PW model is not as straightforward as that for the LWR model. There are similar schemes in the literature that can be used to approximate the PW model, one of which is Roe's flux splitting scheme (*14*). The approximation of Equation 6 using this scheme is:

$$U_i^{j+1} = U_i^j - \frac{k}{h}\left[F_{i+1/2}^j - F_{i-1/2}^j\right] + \frac{k}{2}\left[\hat{s}_{i+1/2}^j + \hat{s}_{i-1/2}^j\right]$$

$$F_{i+1/2}^j = \frac{1}{2}\left\{F_{i+1}^j + F_i^j - \sum_{m=1}^{2}\left[|\hat{\lambda}|_m(\hat{\alpha}_m + \hat{\beta}_m)\hat{e}_m\right]_{i+1/2}^j\right\}$$

Here, $\hat{\lambda}$ and $\hat{e}$ are eigenvalues and eigenvectors of the flux Jacobian $\partial_U F$ in Equation 6, and $\hat{\alpha}$, $\hat{\beta}$, $\hat{s}$ are computed from U_i^j, and U_{i+1}^j.

It should be noted that both the Godunov and Roe schemes can capture shocks sharply and are first-order-accurate and nonoscillating. These numerical schemes are well documented in the literature, and minute details of their derivations will not be repeated here. More details may be found elsewhere (*10*, *15–17*).

DISCUSSION OF NUMERICAL RESULTS

The finite difference schemes in the previous section are used to solve both the LWR and PW models with the sets of Riemann initial data (Rid) shown in Table 1. The units of these initial conditions are speed in miles per hour and density in vehicles per minute. Because the LWR model does not allow travel speed to differ from equilibrium speed, only initial densities were used in computations of LWR solutions. Moreover, natural boundary conditions (i.e., boundary data take the values of density and speed of the immediate neighbor cell within the boundary) were used to ensure that the solutions of both models on a finite road are identical to those that would have been obtained for the same initial conditions on an infinitely long road.

In the numerical computations, a 5-mi (8-km) road was divided into 150 cells; each cell has a length $h = 0.0333$ mi (0.0536 km). The jump location $x = 0$ corresponds with the interface between Cells 75 and 76. Without loss of generality, the simple speed-density relationship of Greenshields (*18*) was used for v_*. Parameters for this relationship are free-flow speed, 60 mph (96.7 km/h); and jam density, 120 vpm (74.5 veh/km). Finally, the time increment k is taken to be 1 s. The reason for choosing such a small value is twofold: (*a*) the CFL condition

$$\max\left|\frac{k}{h}\lambda\right| \le 1$$

must hold to ensure numerical stability (*19*) [λ is the characteristic velocity, $\lambda = f_*'(\rho)$ for LWR and $\lambda = v \pm c_0$ for PW], and (*b*) $k \le \tau$ is required to reduce the stiffness of the relaxation term.

To examine the effects of relaxation on Riemann solutions, for a fixed traffic sound speed [$c_0 = 35$ mph (56 km/h)], different relaxation times ($\tau = 1$ and 30 s) were used to compute Riemann solutions for Rid 1 and 2. When relaxation is fast ($\tau = 1$ s), the Riemann solutions of both models, whether they are shocks or rarefactions or their combinations, are nearly identical (Figure 2). (A minor difference exists: the shocks of the PW solutions oscillate slightly near the shock front. This oscillation is likely to be caused by the stiff relaxation term.) This result confirms the observations of Leo and Pretty (*10*). When relaxation is weaker ($\tau = 30$ s), transient solutions of the PW model differ significantly from those of the LWR model. In the case of Rid 3 (Figure 3*a*), the LWR model simply propagates the shock backward, preserving its form during propagation. The PW model, however, produces a density bulge (which is actually another shock) near the shock front. Owing to relaxation, the bulge spreads and weakens as the shock travels backward, producing a shock front similar to that of the LWR model. Yet the PW shock initially travels noticeably faster than the LWR shock and later, owing to relaxation, adopts the speed of the LWR shock for this set of initial data. In the case of Rid 4 (Figure 3*b*), both models predict traffic dispersion. The PW model appears to have a smaller critical density, yet it discharges traffic more quickly.

Next to be studied is how the strength of anticipation affects Riemann solutions of the PW model. Figure 4 shows Riemann solutions with Rid 3 for different c_0-values [$c_0 = 30$, 35, and 40 mph (48, 56, and 64 km/h)]. It is noted that each of these solutions contains a strong

TABLE 1 Sets of Riemann Initial Data Used

Rid	Initial density	Initial speed
1	$\rho_1(x) = \begin{cases} 50, & x < 0 \\ 90, & x \ge 0 \end{cases}$	$v_1(x) = \begin{cases} v_*(50), & x < 0 \\ v_*(90), & x > 0 \end{cases}$
2	$\rho_2(x) = \begin{cases} 90, & x < 0 \\ 50, & x \ge 0 \end{cases}$	$v_2(x) = \begin{cases} v_*(90), & x < 0 \\ v_*(50), & x > 0 \end{cases}$
3	$\rho_1(x) = \begin{cases} 50, & x < 0 \\ 90, & x \ge 0 \end{cases}$	$v_3(x) = \begin{cases} v_*(50), & x < 0 \\ v_*(90) - 15, & x > 0 \end{cases}$
4	$\rho_2(x) = \begin{cases} 90, & x < 0 \\ 50, & x \ge 0 \end{cases}$	$v_4(x) = \begin{cases} v_*(90), & x < 0 \\ v_*(50) - 10, & x > 0 \end{cases}$

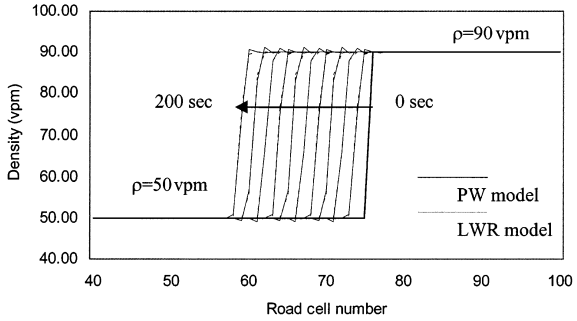

(a) Rid 1

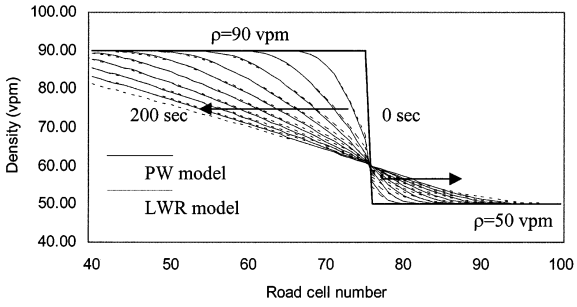

(b) Rid 2

FIGURE 2 Comparison of LWR and PW models ($\tau = 1$ s, $c_0 = 35$ mph) (1 mi = 1.6 km).

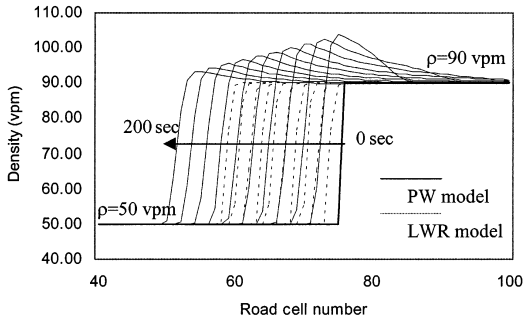

(a) Rid 3

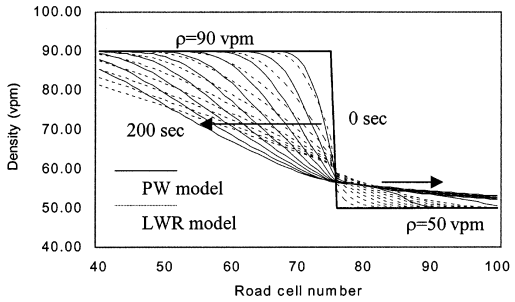

(b) Rid 4

FIGURE 3 Comparison of LWR and PW models (τ = 30 s, c_0 = 35 mph) (1 mi = 1.6 km).

initial shock. The strength of the shock grows with time when anticipation is weak [corresponding to small c_0 (Figure 4*a*)]. It first grows, then weakens to the original level when anticipation is medium [c_0 = 35 mph (Figure 4*b*)]. Finally it grows slightly and then weakens to a level lower than the original level of strength when anticipation is strong [c_0 = 40 mph (Figure 4*c*)]. The shock also becomes noticeably smoother when anticipation is stronger. Moreover, the speed of the shock travels faster as anticipation becomes stronger. These results indicate that anticipation has a stabilizing effect on traffic flow. This finding is quite intuitive: as drivers brake sufficiently early in anticipation of traffic slowdowns, more room is available to make the adjustment, hence wider and smoother shock profiles and more stable traffic patterns.

The last set of graphs (Figure 5) depicts Riemann solutions with Rid 4 for various c_0-values. Each of these solutions contains a strong rarefaction wave. Again, congestion dissipates faster with the increase of c_0 because of driver anticipation, which is clearly related to the increase of critical density for larger c_0. Yet there is a baffling result that could not be explained at the moment. In Figure 4*a*, a weaker stationary shock forms near the location of the initial jump, which does not make physical sense. Both model instability and numerical instability were ruled out as causes of this oddity, which led the authors to believe that the special set of initial conditions and parameters might have hit a problem spot in Roe's flux splitting scheme. This issue will be studied further, and findings will be reported at a later time.

CONCLUDING REMARKS

Despite numerous computational works on higher-order models, still little is known about Riemann solutions of LWR and PW models and how relaxation and anticipation affect these solutions. This situation is largely because the majority of these works have either employed primitive numerical schemes in their analyses or focused on numerical solutions with general initial and boundary data that obscured the unique characters of these models.

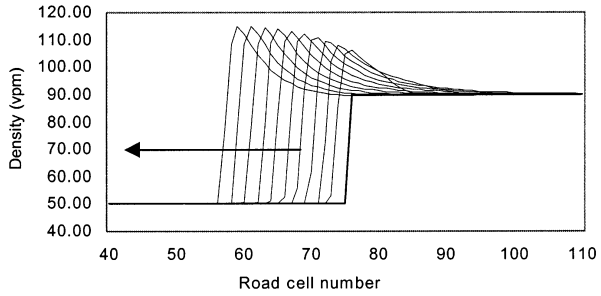

(a) c_0=30 mph

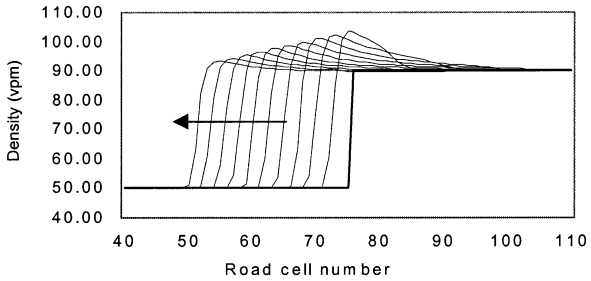

(b) c_0=35 mph

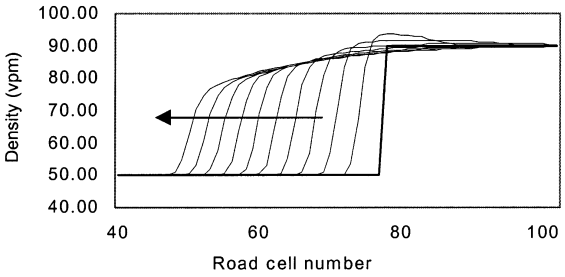

(c) c_0=40 mph

FIGURE 4 PW model with different c_0-values (τ = 30 s, Rid 3) (1 mi = 1.6 km).

In this paper, the Riemann solutions of a particular higher-order model, the PW model, were studied under well-controlled conditions. The Riemann solutions of the PW model with different sets of parameters and Riemann initial data were computed with a shock-capturing numerical scheme—Roe's flux splitting scheme—and compared with the Riemann solutions of the LWR model having the same initial (density) data. It was found that faster relaxation forces the PW model to behave much like the LWR model, that strong anticipation has a stabilizing effect on traffic, and that shock waves travel at different speeds in the PW model than in the LWR model.

To end the paper on a pondering note, there are still some unresolved issues about the PW model despite salient efforts made to understand it. The rarefaction shock encountered in this analysis is

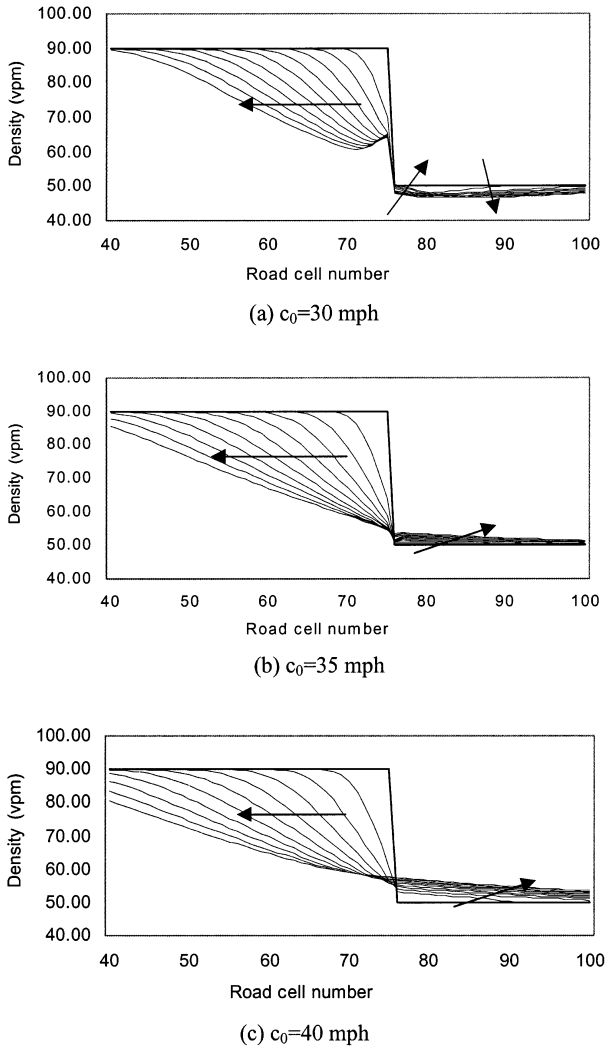

FIGURE 5 PW model with different c_0-values (τ = 30 s, Rid 4) (1 mi = 1.6 km).

one example of such issues. Another example is the occasional appearance of negative states in the PW model. The resolution of these issues, it seems, requires a deeper analysis than blunt computations. Nevertheless, this numerical analysis, limited in scope as it may be, may serve as a stepping stone to a more complete characterization of the properties of PW-like higher-order traffic flow models.

REFERENCES

1. Lighthill, M. J., and G. B. Whitham. On Kinematic Waves II: A Theory of Traffic Flow on Long Crowded Roads. *Proceedings of the Royal Society*, Vol. 229, No. 1178, 1955, pp. 317–345.
2. Richards, P. I. Shock Waves on the Highway. *Operational Research*, Vol. 4, 1956, pp. 42–51.
3. Payne, H. J. Models of Freeway Traffic and Control. In *Mathematical Models of Public Systems* (G.A. Bekey, ed.), Simulation Councils Proceedings Series, Vol. 1, 1971.
4. Whitham, G. B. *Linear and Nonlinear Waves*. John Wiley & Sons, New York, 1974.
5. Papageorgiou, M. *Applications of Automatic Control Concepts to Traffic Flow Modeling and Control*. Lecture Notes in Control and Information Sciences (A.V. Balakrishnan and M. Thoma, eds.), Springer-Verlag, 1983.
6. Papageorgiou, M., J. Blosseville, and H. Hadj-Salem. Modeling and Real-Time Control of Traffic Flow on the Southern Part of Boulevard Peripherique in Paris: Part I: Modeling. *Transportation Research A*, Vol. 24, No. 5, 1990, pp. 345–359.
7. Hauer, E., and V. F. Hurdle. Discussion. In Payne, H. J., FREFLO: A Macroscopic Simulation Model of Freeway Traffic, *Transportation Research Record 722*, TRB, National Research Council, Washington, D.C., 1979, pp. 75–76.
8. Derzko, N. A., A. J. Ugge, and E. R. Case. Evaluation of Dynamic Freeway Flow Model by Using Field Data. In *Transportation Research Record 905*, TRB, National Research Council, Washington, D.C., 1983, pp. 52–60.
9. Daganzo, C. F. Requiem for Second-Order Approximations of Traffic Flow. *Transportation Research B*, Vol. 29, No. 4, 1995, pp. 277–286.
10. Leo, C. J., and R. L. Pretty. Numerical Simulation of Macroscopic Continuum Traffic Models. *Transportation Research B*, Vol. 26, No. 3, 1992, pp. 207–220.
11. Zhang, H. M. An Analysis of the Stability and Wave Properties of a New Continuum Theory. *Transportation Research B,* Vol. 33, No. 6, 1999, pp. 387–398.
12. Courant, R., and K. O. Friedrichs. *Supersonic Flow and Shock Waves*. Interscience, New York, 1948.
13. Godunov, S. K. *Mat. Sbornik*, Vol. 47, 1959, pp. 271–306.
14. Roe, P. L. Approximate Riemann Solvers, Parameter Vectors and Difference Schemes. *Journal of Computational Physics*, Vol. 43, 1981, pp. 357–372.
15. Bui, D. D., S. L. Narasimhan, and P. Nelson. *Computational Realizations of the Entropy Condition in Modeling Congested Traffic Flow*. Report FHWA/TX-92/1232-7. FHWA, U.S. Department of Transportation, 1992
16. Daganzo, C. F. A Finite Difference Approximation of the Kinematic Wave Model of Traffic Flow. *Transportation Research B*, Vol. 29, No. 4, 1995, pp. 261–276.
17. Lebacque, J. P. The Godunov Scheme and What It Means for the First Order Traffic Flow Models. *Proc., Thirteenth International Symposium on Transportation and Traffic Theory*, 1996.
18. Greenshields, B. D. A Study of Traffic Capacity. *HRB Proc.*, Vol. 14, 1934, pp. 448–477.
19. LeVeque, R. *Numerical Methods for Conservation Laws*. Birkhauser Verlag, 1992.

Publication of this paper sponsored by Committee on Traffic Flow Theory and Characteristics.